Available online at www.sciencedirect.com
SCIENCE DIRECT®
Journal of Molecular Catalysis B: Enzymatic 35 (2005) 62–69
JOURNAL OF MOLECULAR CATALYSIS B: ENZYMATIC
www.elsevier.com/locate/molcatb

The modelling and kinetic investigation of the lipase-catalysed acetylation of stereoisomeric prostaglandins

Imre Vallikivi [a,*], Linda Fransson [b], Karl Hult [b], Ivar Järving [a], Tõnis Pehk [c], Nigulas Samel [a], Vello Tõugu [d], Ly Villo [a], Omar Parve [a]

[a] *Department of Chemistry, Tallinn University of Technology, Akadeemia tee 15, 12618 Tallinn, Estonia*
[b] *Department of Biotechnology, Royal Institute of Technology, AlbaNova University Center, SE-10691 Stockholm, Sweden*
[c] *National Institute of Chemical Physics and Biophysics, Akadeemia tee 23, 12618 Tallinn, Estonia*
[d] *Department of Gene Technology, Tallinn University of Technology, Akadeemia tee 15, 12618 Tallinn, Estonia*

Received 8 July 2004; received in revised form 13 May 2005; accepted 18 May 2005

Abstract

The lipase-catalysed acetylation of the hydroxyl groups of five stereoisomeric prostaglandins of type F was investigated by means of molecular dynamics simulations and the results compared with experimental observations. An NMR spectroscopic monitoring was performed to estimate reaction velocities and the regioselectivity. A molecular modelling protocol that could qualitatively differentiate between the OH groups of prostaglandins being either accessible or unaccessible to the *Candida antarctica* lipase B (CALB) catalysed acetylation was developed. The protocol developed analysed the protein structure deformation, the content of essential hydrogen bonds and the function-based subset energy of tetrahedral intermediates along the molecular dynamics simulations trajectory. The tetrahedral intermediates displaying a deformation RMS value lower than 3.0 Å, an essential hydrogen bond content over 50% and a subset energy less than −95 kJ/mol were classified active. In total, the accessibility of 16 out of 17 different prostaglandin OH groups was correctly predicted.
© 2005 Elsevier B.V. All rights reserved.

Keywords: Lipase-catalysed acetylation; Novozym 435; Low-water media; Monitoring by ^{1}H NMR; Prostaglandin; Molecular dynamics simulations

1. Introduction

Several prostaglandins (PG) are currently used as medicines and many more are being subjected to extensive biological and medical research. In the last years, much attention has also been paid to the synthesis and research of prostaglandin-like compounds, the isoprostane derivatives [1–3].

Lipase-catalytic methods have been used for separation of prostanoid enantiomers by kinetic resolution [4–8]. The application of lipase-catalysed reactions to the regio- and chemoselective protection of prostaglandins in the semisynthesis of prostanoids has been described [9]. In the case of the above applications, it is important for a user of lipase-catalytic methods to be able to prognosticate the regio- and stereoselectivity of the reaction.

Several successful applications of molecular modelling methods to the prediction of lipase stereo- and regioselectivity have been described [10–15]. Due to the rapid development of software and hardware in the last decades these predictions can be made relatively fast and with good results.

$PGF_{2\alpha}$ is a well-known bioactive compound, which is used in human and veterinary medicine. It causes the contraction of vascular, bronchial, intestinal and myometrial smooth muscles, and also exhibits a potent luteolytic activity [16]. The physiological activity of $PGF_{2\alpha}$ stereoisomers (15*R*)-$PGF_{2\alpha}$, $PGF_{2\beta}$ and (15*R*)-$PGF_{2\beta}$ have also been described [17]. The isoprostane derivative 8-*iso*-$PGF_{2\alpha}$ has been recently described as a vaso- and bronchoconstrictor and a partial antagonist of the thromboxane receptor in

* Corresponding author. Tel.: +372 6204382; fax: +372 6202828.
E-mail address: imre@chemnet.ee (I. Vallikivi).

1381-1177/$ – see front matter © 2005 Elsevier B.V. All rights reserved.
doi:10.1016/j.molcatb.2005.05.008

platelets. In human whole blood, 8-*iso*-$PGF_{2\alpha}$ exhibits an anti-aggregatory activity [18,19].

In this work, the *Candida antarctica* lipase B (CALB) catalysed acetylation of the above five stereoisomeric prostaglandins of type F was investigated by using molecular dynamics simulation methods in order to characterize the behaviour of the tetrahedral intermediates formed in the active site of the CALB by each of the PG hydroxyl groups. The NMR monitoring of the acetylation of stereoisomeric prostaglandins was performed to estimate the reaction velocities and to determine the regioselectivity. The modelling of tetrahedral intermediates gave characteristics that were further correlated with the experimental data to give quantitative criteria, which could allow testing the accessibility of the hydroxyl groups of related prostanoids to the acetylation catalysed by the CALB.

2. Experimental

2.1. Materials

$PGF_{2\alpha}$ and its stereoisomers were a kind gift from Kevelt Ltd. (Tallinn). The solvents used were purchased from Merck and Aldrich. The immobilised preparation of the *C. antarctica* lipase B (Novozym 435, batch LC2 00015: the declared activity of approximately 7000 PLU/g and water content of 1–2%, w/w) was a generous gift from Novozymes A/S.

2.2. Methods

The ^{1}H and ^{13}C NMR spectra were recorded on a Bruker AMX-500 Spectrometer. The products were identified by performing a full assignment of ^{1}H and ^{13}C chemical shifts by using ^{1}H–^{1}H and ^{1}H–^{13}C 2D COSY correlation diagrams (Table 1).

2.2.1. Lipase-catalysed acetylation

The PG sample was dissolved in deutero acetone (28 μmol/ml) and introduced into a 5 mm NMR tube. Vinyl acetate (20 equivalents in relation to the starting PG) and lipase (20 mg/ml) were added to the mixture. The reaction mixture was stored at room temperature ($20 \pm 2\,^{\circ}C$) without agitation (only the shaking before NMR experiments was performed) [20]. The reaction conditions and the products are presented in Table 2.

The reaction progress was recorded by integrating the peak areas corresponding to the signals of the hydrogen atoms attached to C_{11} 3.8–4.0 ppm (CHOAc) and C_9 4.0–4.1 ppm (CHOAc) of the prostaglandin. The integration results were standardised against an integrated signal (at 0.88 ppm) of the hydrogen atoms of the terminal methyl group of the prostaglandin molecule. The latter value corresponds to the total amount of the prostaglandin and its derivatives in the system.

The apparent second-order rate constants (k_{II}, Table 2) of the acetylation were calculated from the pseudo first-order kinetic curves using the least squares method with the KyPlot program [21]. The initial rates (μmol/(min mg Novozym 435), Table 2) were also calculated (estimated) using the first three to five points of the kinetic curves.

All the reaction products were identified using ^{13}C NMR spectroscopy (Table 1).

2.2.2. Molecular modelling procedure

The molecular modelling procedure used was similar to that reported by Raza et al. [11]. The molecular modelling was based on the crystal structure of the CALB (structure 1TCA [22] acquired from the Protein Data Bank [23]). The two *N*-acetyl-D-glycosamine moieties in the free CALB structure were removed. The hydrogen atoms were added to the heavy atoms and the structure was allowed to relax in the force field. All the hydrogen atoms of the enzyme molecule were allowed to move during a dynamics simulation of 1 ps in length. The energy of the hydrogen atoms in the latter structure was minimised. The above steps were repeated for the water hydrogen atoms. Then, the energy of all the hydrogen atoms was minimised and, finally, the energy of all the atoms was minimised. After that four water molecules were removed from the active site cavity and replaced with a built substrate (PG with an acetyl moiety) covalently bound to Ser 105. The tetrahedral intermediate form of the substrate was manually modelled on the basis of the crystal structure of the CALB with the phosphonate inhibitor (structure 1LBS [24] acquired from the Protein Data Bank [23]). Asp 134 in the acyl binding pocket and the catalytic histidine (His 224) were defined as protonated. The enzyme–substrate system was described using the *Kollman All Atom* force field [25,26]. A non-bonded cut-off distance of 8 Å and a distance-dependent dielectric function with a scaling factor of 1 were used in all calculations. An NTV ensemble (i.e., the constant number of atoms, temperature and volume) and a temperature of 300 K (aside from a short warm-up phase) were used in all molecular dynamics simulations.

Energy minimisations were performed by using the Powell method [27]. The substrates were assigned empirical charges by using the Pullman method [28] (with a formal charge of "−1" for the substrate oxyanion) and the atom types consistent with the force field. The non-standard *Kollman All Atom* force field parameters were assigned analogously to the existing parameters for the angle bending as follows: (1) OS-CT-OS, 109.5°, force constant 250 kJ mol^{-1} $degree^{-2}$; (2) CT-CT-OH, 109.5°, force constant 250 kJ mol^{-1} $degree^{-2}$; (3) C2-CT-OS, 109.5°, force constant 250 kJ mol^{-1} $degree^{-2}$. The substrate was allowed to relax in the enzyme through repeated dynamics simulations and minimisations on the subgroups of the substrates. The minimised structures were used as starting points for dynamics simulations that lasted for 100 ps each. In the final dynamics simulations, all the atoms were allowed to move. The structure was heated up to 300 K by 50 K per 2 ps that resulted in a total heating time of 10 ps. The sample structures were recorded every 0.2 ps in each simulation. The analyses were performed in the last 50 ps of

Table 1
^{13}C NMR chemical shifts of acetylation products (the chemical shifts of 11-acetyl-PGF$_{2\alpha}$ are given in [9])

	8-*iso*-11-Acetyl-PGF$_{2\alpha}$ (**7**)	11-Acetyl-PGF$_{2\beta}$ (**8**)	9-Acetyl-PGF$_{2\beta}$ (**9**)	9,11-Diacetyl-PGF$_{2\beta}$ (**10**)	(15*R*)-11-Acetyl-PGF$_{2\alpha}$ (**11**)	(15*R*)-11-Acetyl-PGF$_{2\beta}$ (**12**)	(15*R*)-9-Acetyl-PGF$_{2\beta}$ (**13**)	(15*R*)-9,11-Diacetyl-PGF$_{2\beta}$ (**14**)
C_1	177.4	177.2	177.4	177.3	176.7	176.9	176.9	176.9
C_2	32.8	33.0	33.0	33.0	32.6	32.9	32.9	32.9
C_3	24.4	24.4	24.4	24.4	24.4	24.5	24.5	24.5
C_4	26.4	26.4	26.3	26.3	26.1	26.3	26.3	26.3
C_5	130.0	130.8	130.4	130.8	130.0	130.3	130.7	130.6
C_6	129.2	127.6	127.4	126.9	128.6	127.4	127.7	127.0
C_7	26.8	28.6	29.2	28.5	24.5	28.7	29.0	28.5
C_8	50.3	51.7	48.9	48.3	50.0	51.9	49.2	48.5
C_9	75.7	72.5	76.5	76.1	71.5	74.8	76.6	76.3
C_{10}	40.0	39.9	39.9	37.6	41.0	40.2	40.1	37.7
C_{11}	77.5	76.9	75.4	74.8	78.8	76.4	75.2	76.1
C_{12}	49.7	52.3	55.6	51.6	51.6	52.8	55.8	52.2
C_{13}	127.3	131.9	131.9	131.9	132.0	131.7	131.7	131.7
C_{14}	135.5	134.7	135.8	135.1	135.3	135.1	135.9	135.7
C_{15}	72.6	72.5	73.0	72.4	73.3	72.9	73.0	73.1
C_{16}	37.0	37.0	37.0	36.9	37.1	37.0	37.1	37.0
C_{17}	25.0	25.0	25.2	25.0	25.0	25.0	25.1	25.0
C_{18}	31.7	31.7	31.7	31.7	31.6	31.7	31.7	31.7
C_{19}	22.6	22.6	22.6	22.6	22.6	22.6	22.6	22.6
C_{20}	14.0	14.0	14.0	14.0	14.0	14.0	14.0	14.0
$C_{9'}$	–	–	170.7	170.8	–	–	170.6	170.6
$C_{9''}$	–	–	21.2	21.2	–	–	21.2	21.2
$C_{11'}$	170.9	170.9	–	170.9	170.8	170.6	–	170.6
$C_{11''}$	21.3	21.1	–	21.1	21.1	21.0	–	20.9

Table 2
The CALB-catalysed acetylation of $PGF_{2\alpha}$ and its stereoisomers

Substrate (mg)	Time of monitoring[a] (h)	Degree of conversion (%)	Apparent second-order rate constant $k_{II} \pm$ S.E. (min^{-1} $(g/ml)^{-1}$)	Estimated initial rate[b] (μmol/(min mg Novozym 435))	Products (ratio)
$PGF_{2\alpha}$ (**1**), 10	25	99	0.31 ± 0.03	0.64	(**6**)
8-*iso*-$PGF_{2\alpha}$ (**2**), 9	120	85	0.022 ± 0.005	0.11	(**7**)
$PGF_{2\beta}$ (**3**), 9	11	95	0.285 ± 0.054	0.81	(**8**)/(**9**)/(**10**) (1/2/0.75)
(15*R*)-$PGF_{2\alpha}$ (**4**), 7	22	95	0.090 ± 0.008	0.16	(**11**)
(15*R*)-$PGF_{2\beta}$ (**5**), 8	21	95	0.22 ± 0.07	0.34	(**12**)/(**13**)/(**14**) (1/1/0.75)

[a] During monitoring 6–10 NMR measurements were performed to give a kinetic curve from which the apparent second-order rate constant (k_{II}) value was calculated.
[b] Relative errors were estimated to be ±20%.

each simulation, giving altogether 250 non-minimised structures for each PG/enzyme system. All the modelling was performed using a SYBYL 6.7 software package [29] on a SGI Octane UNIX workstation.

3. Results and discussion

3.1. The CALB-catalysed acetylation of isomeric prostaglandins

The CALB-catalysed acetylation of $PGF_{2\alpha}$ and its stereoisomers (Scheme 1) was monitored by using ^{1}H NMR spectroscopy. The consumption of prostaglandins followed the pseudo-first-order kinetics suggesting that there is no extensive complex formation of PG with the lipase before its nucleophilic attack to the acyl-enzyme. The apparent second-order rate constants (k_{II}) and the initial rates of acetylation reactions were calculated (Table 2).

For all isomers the C_{11}-OH group was acetylated at a significant rate. The C_{15}-OH group was either inaccessible to the CALB or acetylated at a rate more than two orders of magnitude lower than that of the C_{11}-OH group of the corresponding PG (Table 3). The C_9-OH group was acetylated only in the case of (9*R*)-stereoisomers. The C_9-OH groups of $PGF_{2\beta}$ and (15*R*)-$PGF_{2\beta}$ were acetylated at a significant

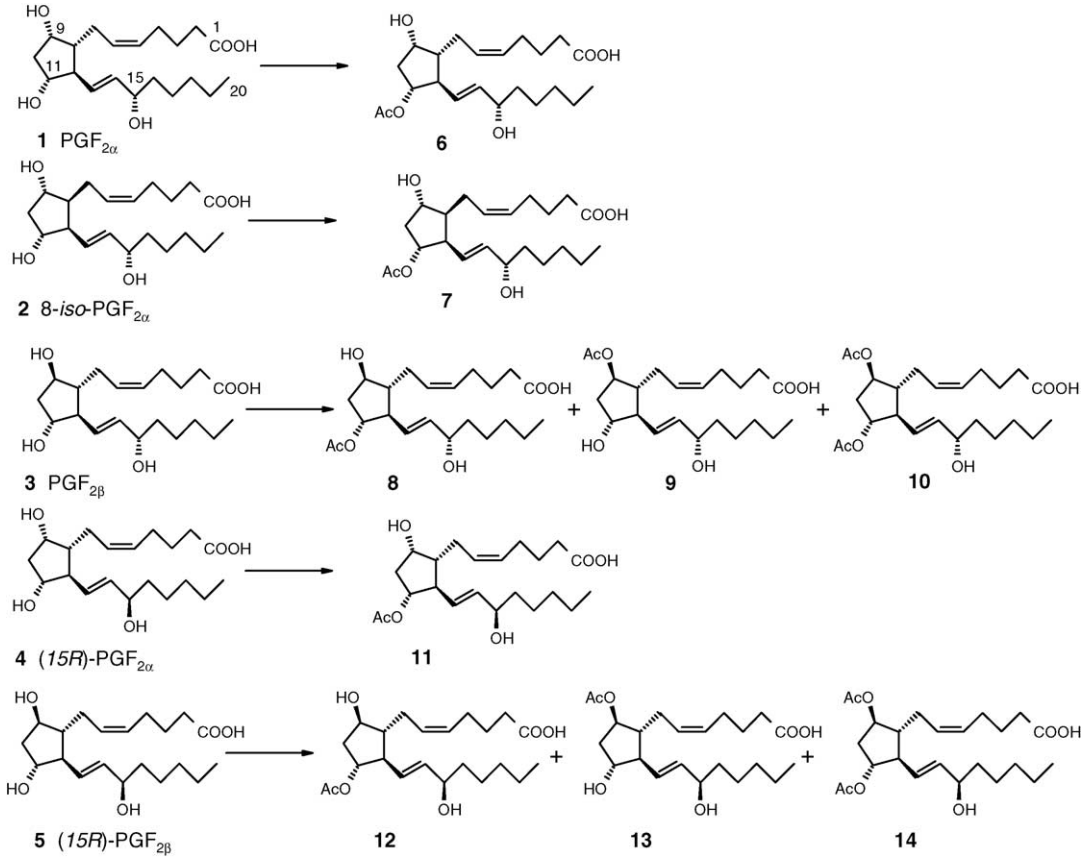

Scheme 1. The CALB-catalysed acetylation of $PGF_{2\alpha}$ and its stereoisomers.

Table 3
The characteristics of $PGF_{2\alpha}$ and its stereoisomers found by means of molecular dynamics calculations

Substance	Acetylated OH group	Potential energy[a] (kJ/mol)	Energy of function-based subset[b] (kJ/mol)	Essential hydrogen bond (%)[b,c]	Deformation RMS[d] (Å)	k_{II} experimental ($min^{-1}(g/ml)^{-1}$)	Estimated initial rate (μmol/(min mg Novozym 435))
$PGF_{2\alpha}$ (**1**)	9	−22 430	**−93**	**25**	1.4	n.o.[e]	n.o.[e]
	11	−22 470	−101	73	1.4	0.31	0.64
	15	−22 640	−103	74	**5.3**	n.o.[e]	n.o.[e]
8-*iso*-$PGF_{2\alpha}$ (**2**)	11	−22 400	−103	64	1.6	0.022	0.11
$PGF_{2\beta}$ (**3**)	9	−22 510	−103	81	1.8	0.19	0.54
	11	−22 470	−98	56	1.4	0.095	0.27
	15	−22 550	−105	90	**5.6**	n.o.[e]	n.o.[e]
(15*R*)-$PGF_{2\alpha}$ (**4**)	9	−22 340	**−92**	**24**	1.2	n.o.[e]	n.o.[e]
	11	−22 300	−100	79	1.1	0.09	0.16
	15	−22 640	**−94**	77	1.6	n.o.[e]	n.o.[e]
(15*R*)-$PGF_{2\beta}$ (**5**)	9	−22 670	−97	70	1.3	0.11	0.17
	11	−22 260	−102	87	2.1	0.11	0.17
	15	−22 890	−101	83	**2.6**	n.o.[e]	n.o.[e]

The values indicating the inaccessibility of the OH group to the CALB-catalysed acetylation according to the modelling protocol developed have been marked in bold.

[a] A potential energy of the whole system, the mean value calculated for the last 50 ps of molecular dynamics.

[b] See Scheme 2.

[c] The percentage of the bonds between the substrate and the H bond donor groups, including the corresponding hydrogen atoms associated with the tetrahedral centre, namely, His 224:N_ε, Gln 106:N, Thr 40:N and Thr 40:O_γ.

[d] An RMS deviation of the system backbone atoms from their centre of mass, the mean value from the last 50 ps of molecular dynamics.

[e] The formation of the product was not observed, the detection limit was 0.001.

rate (Table 3). Somewhat unexpectedly, the C_9-OH and C_{11}-OH groups of $PGF_{2\beta}$ as well as (15*R*)-$PGF_{2\beta}$ were acetylated without a strict order: both the monoacetates were simultaneously detected in the reaction mixture. This was important for the evaluation of the modelling results described in this work because it gave evidence of an actual competition between the C_9-OH and C_{11}-OH groups as nucleophiles in the acetylation.

In the case of $PGF_{2\beta}$ (15*S*) and (15*R*)-$PGF_{2\beta}$, the stereochemistry of the C_{15}-OH group influences the ratio of regioisomeric acetylation products. The acetylation of $PGF_{2\beta}$ gives 9- and 11-monoacetates at a ratio of 2:1, respectively, while the acetylation of (15*R*)-$PGF_{2\beta}$ affords these products at a ratio of 1:1. In both the cases, the formation of 9,11-diacetate was also observed. In the case of $PGF_{2\alpha}$ (15*S*) and (15*R*)-$PGF_{2\alpha}$ (Table 2), the absolute configuration of the stereogenic centre at the C_{15} carbon atom influences the reaction velocity as well as the C_{11}-OH group of $PGF_{2\alpha}$ was acetylated at a rate three times the rate of acetylation of its (15*R*) counterpart.

The C_{11}-OH group of 8-*iso*-$PGF_{2\alpha}$, which, in comparison with $PGF_{2\alpha}$, has an opposite configuration at C_8, was acetylated at a rate approximately tenfold lower than $PGF_{2\alpha}$. Our previous results have demonstrated the decisive role of interactions between the PG carboxyl group (versus the corresponding methyl ester) and the functional groups of the active site region of the CALB, for instance, in enabling the acetylation of the C_{15}-OH group of PGs. Consequently, both the steric and non-steric interactions occurring simultaneously may lead to a lower rate of 8-*iso*-$PGF_{2\alpha}$ acetylation.

3.2. Molecular modelling of the CALB-catalysed acetylation of stereoisomeric PGs

Structurally similar prostaglandins behave differently in the active site of lipases. In this work, we investigated the behaviour of $PGF_{2\alpha}$ and its stereoisomers (compounds **1–5**) in the active site of the CALB. The objective was to work out a computational method to test the accessibility of the hydroxyl groups of prostanoids to the CALB-catalysed acetylation. The resulting procedure would present a way to predict the stereo- and regioselectivity of the CALB-catalysed acetylation of prostaglandins.

The modelling procedure was based upon molecular dynamics simulations of tetrahedral intermediates (Scheme 2) in order to give a sampling of the enzyme–substrate conformational space. The tetrahedral intermediates of acetyl esters

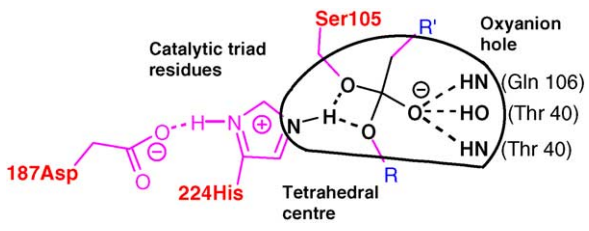

Scheme 2. The catalytic triad in the CALB with a substrate forming a tetrahedral intermediate. The atoms marked in black participate in the function-based subset of the enzyme. The hydrogen bonds essential for catalysis have been drawn in black. For a structure to be considered active both hydrogen bonds from histidine, and at least two hydrogen bonds to the carbonyl oxygen out of three should be present.

formed with the alcohol group attached to C_9, C_{11} and C_{15}, respectively, for four prostaglandins (**1, 3–5**) and the acetyl ester formed with the alcohol group attached to the C_{11} of 8-*iso*-$PGF_{2\alpha}$ (**2**) were studied. Altogether 13 different 100 ps molecular dynamics runs were performed. The last 50 ps of the dynamics runs were evaluated in the following four ways, by using:

(1) a potential energy of the whole system, the mean value of all structures from the last 50 ps of the dynamics simulation;
(2) the function-based subset energy as defined by Raza et al. [11] and shown in Scheme 2, the mean value of all structures from the last 50 ps of the dynamics simulation;
(3) the percentage of structures having hydrogen bonds essential for the catalytic process (see Scheme 2);
(4) an average degree of deformation, the "deformation RMS" calculated as a root mean square (RMS) deviation of the enzyme from the initial structure.

These analyses were compared with experimentally estimated initial rates (and apparent second-order rate constants) for each acylation product.

The results of all calculations are presented in Table 3.

For the 13 enzyme–substrate complexes studied, the deformation RMS varied between 1.1 and 5.6 Å. The degree of deformation was related to the alcohol group used in ester formation. For each prostaglandin studied, the deformation RMS values of the esters connected to C_{15} were the highest. This observation was in accordance with experimental determinations where no remarkable formation of C_{15}-esters was observed. In two cases, $PGF_{2\alpha}$ (**1**) and $PGF_{2\beta}$ (**3**), the enzyme became visually distorted with a deformation RMS of over 5 Å. In the third case, (15*R*)-$PGF_{2\beta}$ (**5**), the deformation was still high, 2.6 Å, although the overall enzyme conformation remained intact. The tetrahedral intermediates involving prostaglandins over the C_9- and C_{11}-OH groups were more similar in deformation RMS. The RMS deformation values calculated for them were below 2 Å, except for the C_{11}-OH group of (15*R*)-$PGF_{2\beta}$, in case of which it was 2.1 Å.

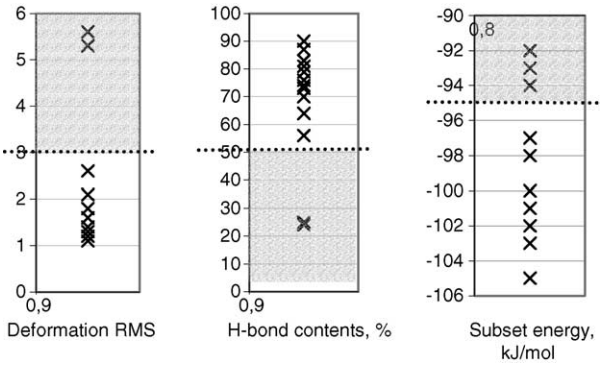

Fig. 1. The distribution of deformation RMS, hydrogen bond contents and subset energy for the 13 OH groups of prostaglandins tested. The suggested limits between the reactive and unreactive complexes are marked with dotted lines. The grey area marks unacceptable values.

The hydrogen bond contents of the 13 enzyme–substrate complexes studied varied between 24 and 90%. The hydrogen bonds percentage of two complexes was less than 50%; both the complexes were C_9-acetates, one of $PGF_{2\alpha}$ (**1**), the other, of (15*R*)-$PGF_{2\alpha}$ (**4**).

The function-based subset energy varied between −105 and −92 kJ/mol. Two, C_9-acetates, $PGF_{2\alpha}$ (**1**) and (15*R*)-

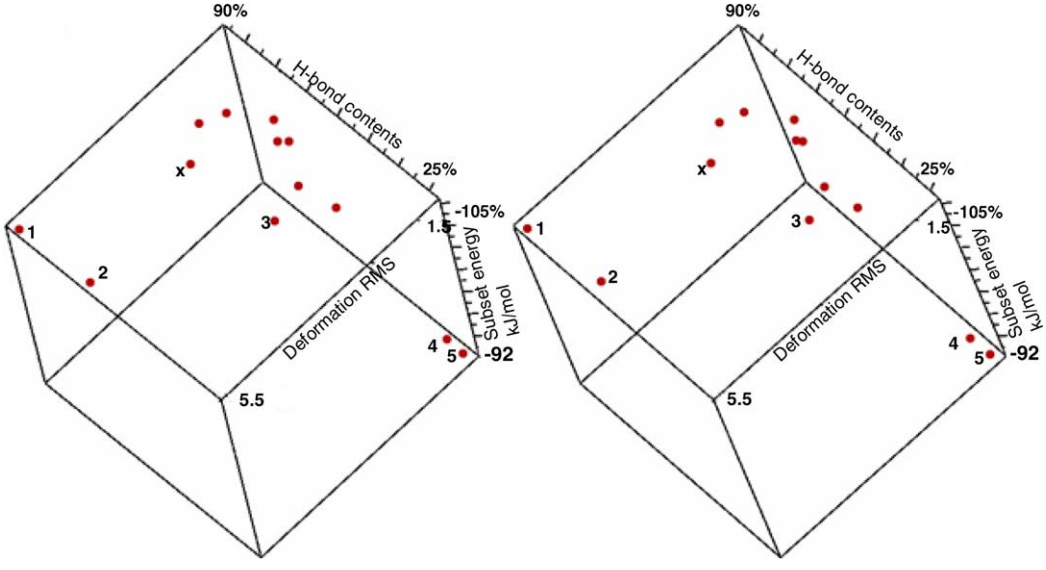

Fig. 2. A stereo view of the 3D distribution of the modelling parameters studied. The unreactive enzyme–substrate complexes are marked with numbers 1–5. 'x' denotes a false positive structure. (1) $PGF_{2\beta}$ (**3**), C_{15}-acetate. Violated criterion: deformation RMS. (2) $PGF_{2\alpha}$ (**1**), C_{15}-acetate. Violated criterion: deformation RMS. (3) (15*R*)-$PGF_{2\alpha}$ (**4**), C_{15}-acetate. Violated criterion: subset energy. (4) $PGF_{2\alpha}$ (**1**), C_9-acetate. Violated criterion: subset energy and hydrogen bond contents. (5) (15*R*)-$PGF_{2\alpha}$ (**4**), C_9-acetate. Violated criterion: subset energy and hydrogen bond contents. (x) The false positive structure, (15*R*)-$PGF_{2\beta}$ (**5**), C_{15}-acetate. (Violated criterion: deformation RMS?).

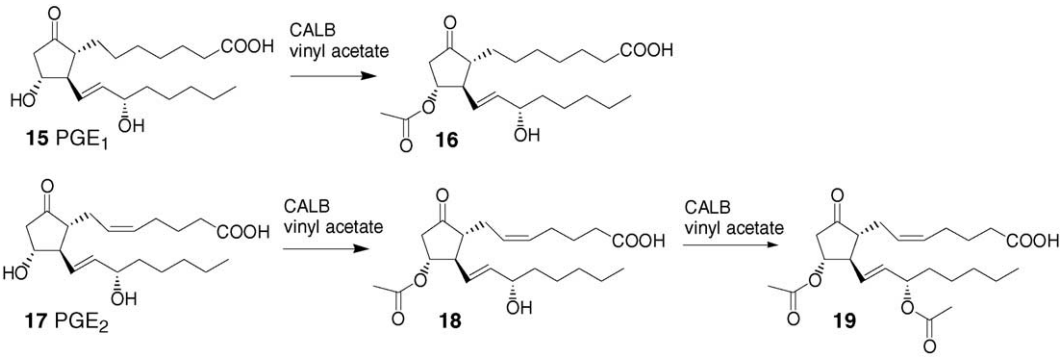

Scheme 3. The CALB-catalysed acetylation of PGE_1 (**15**) and PGE_2 (**17**). No C_{15}-monoacetates were detected aside from C_{11}-monoacetates in the acetylation mixtures.

$PGF_{2\alpha}$ (**4**), displayed the highest energies, −93 and −92 kJ/mol, respectively. The energy of one C_{15}-acetate, (15*R*)-$PGF_{2\alpha}$ (**4**), was −94 kJ/mol. The total potential energy is tabulated for reference. The small variations in the potential energy of the systems are far too large in absolute value and too sensitive at the same time to be used in a modelling protocol of this type. The potential energy is very sensitive to distant changes in the structures, for example, to the rearrangement of water molecules or water hydrogen bonds, adding a significant noise contribution to the signal.

3.2.1. The construction of the modelling protocol

The distribution of experimental data was studied to propose a modelling protocol. For the three parameters studied, viz. deformation RMS, hydrogen bond content and subset energy, limits were set to the gaps of data distribution (Fig. 1). The proposed limits were:

- deformation RMS of 3 Å;
- hydrogen bond contents of 50%;
- function-based subset energy of −95 kJ/mol.

The violation of any of these three parameters would be indicative of an OH group of a prostaglandin non-accessible to the CALB-catalysed acetylation (an "unreactive OH group"). The experiments showed that out of the 13 OH groups studied, seven were reactive and six unreactive or virtually unreactive. We classified C_{15}-OH groups as "virtually unreactive" because they were acetylated partially, at a very low rate, only after the C_{11}-OH group was acetylated [9,20]. With the suggested modelling protocol all the OH groups of prostaglandins accessible to the CALB-catalysed acetylation were correctly predicted as reactive and out of the six non-reacting OH groups of prostaglandins five, were correctly predicted as unreactive. In Fig. 2, the 3D distribution of the parameters is shown.

The cut-off value of deformation RMS could be considered a lower (about 2.3–2.4 Å), than chosen, 3 Å value. For this, we should ignore the virtual borders of the compact separated clusters of the values. The experimental proved that the lowest deformation RMS value indicative of unreactivity of an OH group was as low as 2.6 Å (C_{15}-OH of (15*R*)-$PGF_{2\beta}$ (**5**)). At the same time, this is the highest value (next to the value 2.1 Å, that characterizes accessible to the CALB C_{11}-OH group of (15*R*)-$PGF_{2\beta}$ (**5**)) in the cluster involving values that belong to the reactive OH groups.

In order to evaluate the constructed protocol, a further two prostaglandins were studied and evaluated.

3.2.2. Evaluation of the modelling protocol

To evaluate the modelling protocol, two prostaglandins were tested additionally. These were PGE_1 (**15**) and PGE_2 (**17**) (Scheme 3), both of them with ester bonds at either position C_{11} or C_{15}. The experimental and modelling results are presented in Table 4.

Table 4
The characteristics of PGE_1 (**15**) and PGE_2 (**17**) found by means of molecular dynamics calculations

Substance	Acetylated OH group	Potential energy[a] (kJ/mol)	Energy of function-based subset[a] (kJ/mol)	Essential hydrogen bond (%)[a]	Deformation RMS[a]	Possibility of acetylation reaction
PGE_1 (**15**)	11	−22300	−96	85	1.7	Yes[b]
	15	−22250	−99	92	**3.6**	No[b]
PGE_2 (**17**)	11	−22660	−96	65	1.8	Yes[c]
	15	−22430	**−83**	**25**	1.2	No[c]

The values indicating unaccessibility of an OH group to the CALB-catalysed acetylation according to the modelling protocol developed are marked in bold.

[a] See Table 3.

[b] The acetylation of the C_{11}-OH group of PGE_1 is possible, the C_{15}-OH group was not acetylated [9].

[c] The acetylation of the C_{11}-OH group of PGE_2 has been shown to proceed at a lower rate than that of $PGF_{2\alpha}$; the C_{15}-OH group of PGE_2 was acetylated only after the acetylation of the C_{11}-OH group [20]. Consequently, the results of calculations presented, e.g. the acetylation of the C_{15}-OH group of prostaglandins are not relevant in this case.

Two of the four-modelled acetates fell outside the criteria for an active ester intermediate: the PGE_1 C_{15}-acetate showed too high a deformation RMS (3.6 Å) and the PGE_2 C_{15}-acetate had too high a subset energy (−83 kJ/mol). The C_{11}-OH groups of prostaglandins were predicted to be reactive; this was in agreement with experimental results [20].

In total, out of the 17 tested prostaglandin OH groups the protocol managed to correctly predict the possibility of acetylation of 16 with the CALB.

4. Conclusions

We presented a protocol to determine the accessibility of the OH groups of prostaglandins to the acetylation catalysed with the CALB. The protocol was based on a combination of geometrical and energetical considerations, viz. deformation RMS, hydrogen bond contents in the reaction centre and subset energy of atoms central in the transition state complex. With cut-off limits defined from the distribution of 13 test complexes, 12 structures were correctly predicted as reactive/unreactive. A further test-set of acetylation of four OH groups of E type prostaglandins was studied. For all of them, the reactivity was correctly predicted.

Although the limits to the modelling parameters used—deformation RMS, hydrogen bond contents and subset energy, were set ad hoc, the combination of the parameters studied was not. In the modelling, we started from an artificially built transition state analog, which may actually be impossible to reach, and this is the structure we have to evaluate.

The three parameters—deformation RMS, hydrogen bond ratio and subset energy, can be visualised as the three filters a structure has to pass in order to be considered reactive. The RMS deviation "filter" removes the constructed transition state structures that actually cannot exist. For them, the complex is too cramped, the space is too limited or there are too severe interactions between the enzyme and the substrate to allow the enzyme to resolve the problems without distortion. The structures that pass the RMS deviation filter are structures that (a) can exist and are checked for their hydrogen bond ratio. A full hydrogen bond pattern is needed for the complex to (b) be reactive, and the absence of hydrogen bonds indicates a degree of the non-productive binding. Finally, the reactive structures have also to be likely. This will be taken care of by an energy filter, removing high-energy structures and accepting low-energy (c) probable structures.

One difficulty inherent in the presented methodology is to assure that the constructed starting structure is the best possible or at least good enough. If the modeller is not able to construct a good enzyme–substrate complex, the substrate will be deemed as much worse than it actually is. In order to strengthen the method, a study of the results of repeated simulations is necessary.

Acknowledgements

The authors thank Novozymes A/S for the kind gift of Novozym 435. We also thank the Estonian Ministry of Education and Research (Grant No. 0142498s03) and the Estonian Science Foundation for the financial support (Grants Nos. 4758, 5100, 5133, 5639). I. Vallikivi is grateful for the financial support from Sven och Dagmar Salén Stiftelse and the Swedish Institute (the Visby Programme).

References

[1] D.F. Taber, K. Kanai, J. Org. Chem. 63 (1998) 6607.
[2] D.F. Taber, K. Kanai, J. Org. Chem. 64 (1999) 7983.
[3] A.R. Rodriguez, B.W. Spur, Tetrahedron Lett. 43 (2002) 9249.
[4] D.F. Taber, K. Kanai, Tetrahedron 54 (1998) 11767.
[5] D.F. Taber, K. Kanai, R. Pina, J. Am. Chem. Soc. 121 (1999) 7773.
[6] D.F. Taber, Q. Jiang, J. Org. Chem. 66 (2001) 1876.
[7] D.F. Taber, M. Xu, J.C. Hartnett, J. Am. Chem. Soc. 124 (2002) 13121.
[8] I. Vallikivi, Ü. Lille, A. Lõokene, A. Metsala, P. Sikk, V. Tõugu, H. Vija, L. Villo, O. Parve, J. Mol. Catal. B: Enzym. 22 (2003) 279.
[9] O. Parve, I. Järving, I. Martin, A. Metsala, I. Vallikivi, M. Aidnik, T. Pehk, N. Samel, Bioorg. Med. Chem. Lett. 9 (1999) 1853.
[10] R.J. Kazlauskas, Curr. Opin. Chem. Biol. 4 (2000) 81.
[11] S. Raza, L. Fransson, K. Hult, Protein Sci. 10 (2001) 329.
[12] P. Berglund, I. Vallikivi, L. Fransson, H. Dannacher, M. Holmquist, M. Martinelle, F. Björkling, O. Parve, K. Hult, Tetrahedron: Asymmetry 10 (1999) 4191.
[13] R.T. Otto, H. Scheib, U.T. Bornscheuer, J. Pleiss, C. Syldatk, R.D. Schmid, J. Mol. Catal. B: Enzym. 8 (2000) 201.
[14] S. Tomić, B. Kojić-Prodić, J. Mol. Graph. Model. 21 (2002) 241.
[15] R.W. McCabe, A. Taylor, Enzyme Microb. Technol. 35 (2004) 393.
[16] B. Samuelsson, M. Goldyne, E. Granström, M. Hamberg, S. Hammarstrom, C. Malmsten, Annu. Rev. Biochem. 47 (1978) 997.
[17] W.L. Miller, M.J. Sutton, Prostaglandins 11 (1976) 77.
[18] J.-L. Cracowski, T. Durand, G. Bessard, Trends Pharmacol. Sci. 23 (2002) 360.
[19] J.-L. Cracowski, Chem. Phys. Lipids 128 (2004) 75.
[20] I. Vallikivi, I. Järving, T. Pehk, N. Samel, V. Tõugu, O. Parve, J. Mol. Catal. B: Enzym. 32 (2004) 15.
[21] KyPlot 2.0, KyensLab Incorporated, 2-1-4-412 Sotokanda, Chiyoda-ku, Tokyo 101-0021, Japan.
[22] J. Uppenberg, M.T. Hansen, S. Patkar, T.A. Jones, Structure 2 (1994) 293.
[23] H.M. Berman, J. Westbrook, Z. Feng, G. Gilliland, T.N. Bhat, H. Weissig, I.N. Shindyalov, P.E. Bourne, Nucleic Acid Res. 28 (2000) 235.
[24] J. Uppenberg, N. Öhrner, M. Norin, K. Hult, G.J. Kleywegt, S. Patkar, V. Waagen, T. Anthonsen, T.A. Jones, Biochemistry 34 (1995) 16838.
[25] S.J. Weiner, P.A. Kollman, D.A. Case, U.C. Singh, C. Ghio, G. Alagona, S. Profeta, P. Weiner, J. Am. Chem. Soc. 106 (1984) 765.
[26] S.J. Weiner, P.A. Kollman, D.T. Nguyen, D.A. Case, J. Comput. Chem. 7 (1986) 230.
[27] M.J.D. Powell, Math. Program. 12 (1977) 61.
[28] H. Berthod, A. Pullman, J. Chem. Phys. 62 (1965) 942.
[29] Sybyl 6.7, Tripos Inc., 1699 South Hanley Rd., St. Louis, MO 63144, USA.